JOURNAL OF GEOPHYSICAL RESEARCH, VOL. 105, NO. A8, PAGES 18,675–18,692, AUGUST 1, 2000

Polar spacecraft based comparisons of intense electric fields and Poynting flux near and within the plasma sheet-tail lobe boundary to UVI images: An energy source for the aurora

J. R. Wygant,[1] A. Keiling,[1] C. A. Cattell,[1] M. Johnson,[1] R. L. Lysak,[1] M. Temerin,[2] F. S. Mozer,[2] C. A. Kletzing,[3] J. D. Scudder,[3] W. Peterson,[4] C. T. Russell,[5] G. Parks,[6] M. Brittnacher,[6] G. Germany,[7] and J. Spann [7]

Abstract. In this paper, we present measurements from two passes of the Polar spacecraft of intense electric and magnetic field structures associated with Alfven waves at and within the outer boundary of the plasma sheet at geocentric distances of 4-6 R_E near local midnight. The electric field variations have maximum values exceeding 100 mV/m and are typically polarized approximately normal to the plasma sheet boundary. The electric field structures investigated vary over timescales (in the spacecraft frame) ranging from 1 to 30 s. They are associated with strong magnetic field fluctuations with amplitudes of 10-40 nT which lie predominantly in the plane of the plasma sheet and are perpendicular to the local magnetic field. The Poynting flux associated with the perturbation fields measured at these altitudes is about 1-2 ergs $cm^{-2} s^{-1}$ and is directed along the average magnetic field direction toward the ionosphere. If the measured Poynting flux is mapped to ionospheric altitudes along converging magnetic field lines, the resulting energy flux ranges up to 100 ergs $cm^{-2} s^{-1}$. These strongly enhanced Poynting fluxes appear to occur in layers which are observed when the spacecraft is magnetically conjugate (to within a 1° mapping accuracy) to intense auroral structures as detected by the Polar UV Imager (UVI). The electron energy flux (averaged over a spatial resolution of 0.5°) deposited in the ionosphere due to auroral electron beams as estimated from the intensity in the UVI Lyman-Birge-Hopfield-long filters is 15-30 ergs $cm^{-2} s^{-1}$. Thus there is evidence that these electric field structures provide sufficient Poynting flux to power the acceleration of auroral electrons (as well as the energization of upflowing ions and Joule heating of the ionosphere). During some events the phasing and ratio of the transverse electric and magnetic field variations are consistent with earthward propagation of Alfven surface waves with phase velocities of 4000-10000 km/s. During other events the phase shifts between electric and magnetic fields suggest interference between upward and downward propagating Alfven waves. The E/B ratios are about an order of magnitude larger than typical values of c/Σ_P, where Σ_P is the height integrated Pedersen conductivity . The contribution to the total energy flux at these altitudes from Poynting flux associated with Alfven waves is comparable to or larger than the contribution from the particle energy flux and 1-2 orders of magnitude larger than that estimated from the large-scale steady state convection electric field and field-aligned current system.

1. Introduction

The University of California Berkeley, Electric Field Instrument on the Polar spacecraft provides the opportunity to explore the structure and dynamics of electric fields at the plasma sheet boundary at 4-6 R_E geocentric distance. This region is located at altitudes between the auroral acceleration region at distances of 1.5-3 R_E and the more distant portions of the geomagnetic tail where energy conversion processes associated with reconnection occur. In this paper, we describe the first observations of intense electric and magnetic field fluctuations associated with Alfven waves near the outer boundary of the plasma sheet which have sufficient Poynting flux flowing along magnetic field lines toward the ionosphere to power low-altitude auroral acceleration processes. These observations are obtained from two passes of Polar near local midnight on May 1, 1997 and May 9, 1997. These events were chosen from the 20-30 most intense plasma sheet electric field structures obtained during the ~400 plasma sheet crossings of 1997. These measurements are compared to simultaneous ultraviolet images of the aurora from the Polar Ultraviolet Imager (UVI). The ultraviolet images are used to establish that, near the time of the observations of strong Poynting flux, the spacecraft was on magnetic field lines mapping to regions of

[1]School of Physics and Astronomy, University of Minnesota, Minneapolis.
[2]Space Sciences Laboratory, University of California, Berkeley.
[3]Department of Physics and Astronomy, University of Iowa, Iowa City.
[4]Lockheed-Martin Palo Alto Laboratories, Palo Alto, California.
[5]Institute of Geophysics and Planetary Physics, University of California, Los Angeles.
[6]Geophysics Program, University of Washington, Seattle.
[7]NASA Marshall Space Flight Center, Huntsville, Alabama.

Paper number 1999JA900500.
0148-0227/00/1999JA900500$09.00

strong auroral emission. The images also provide estimates of the energy flux deposited in the auroral ionosphere due to electron beams energized at 1 R_E altitude in the auroral acceleration region. To our knowledge, there has never been an experimental determination of the value of Poynting flux directed toward the Earth at the outer boundary of the plasma sheet above the auroral acceleration region. The measurement of Poynting flux and its comparison to the energy flux associated with auroral electron beams is motivated by the fact that the particle energization processes which take place in the auroral acceleration region (particularly those involving acceleration of electron beams) require a significant fraction of the energy extracted by the Earth's magnetosphere from the solar wind. However, it has not been clear experimentally which specific processes and structures in the geomagnetic tail at altitudes above the auroral acceleration region are responsible for providing this power or how it is transferred to lower altitudes where it is dissipated in auroral particle acceleration and Joule heating of the ionosphere.

A number of lower-altitude spacecraft including S3-3 [*Mozer et al.*, 1977; 1980; *Temerin et al.*, 1981], Viking [*Block and Falthammar*, 1990], DE-1 [*Weimer and Gurnett*, 1993; *Reiff et al.*, 1993], Fast Auroral Snapshot Explorer (FAST) [*Carlson et al*, 1998, *Ergun et al.*, 1998; *McFadden et al.*, 1998], and Polar [*Mozer et al.*, 1997] have explored the auroral acceleration region at geocentric distances between 1.5 and 3.5 R_E on auroral field lines. It is well established that this region is the site of a rich phenomenology of plasma processes which create a wide variety of accelerated particle populations. One of the most important from an energetics standpoint is the acceleration of auroral electron beams by steady state and transient electric fields parallel to the magnetic field.

The relation of Poynting flux measurements at 4-6 R_E altitude to lower-altitude particle acceleration processes may be addressed within the context of the Poynting theorem:

$$\frac{\partial}{\partial t}\left(E^2 + B^2\right)/8\pi + c\nabla\cdot(\vec{E}\times\vec{B})/4\pi = -\vec{J}\cdot\vec{E} = -\frac{\partial K}{\partial t} + -\nabla\cdot F_E$$

where E is the electric field, B is the magnetic field, and J is the electric current density, $J\cdot E$ is the power dissipated per unit volume in the energization of particles, K is the kinetic energy density of the particles, and F_E is the kinetic energy flux. The relevant fields which are used to calculate the Poynting flux are the perturbation electric (δE) and magnetic (δB) fields. In both events presented herein, we have subtracted background fields from the measured fields to determine the perturbation fields. In the context of this paper, these perturbation fields may be due to small scale size steady state electric field structures associated with field-aligned currents which close at lower altitudes. Alternatively, they may be associated with time variable Alfvenic structures. In either of these cases, in the MHD limit, the Poynting flux is directed along the background magnetic field. In the absence of any buildup of significant electromagnetic or particle energy density between 1 and 5 R_E on auroral field lines, we have in steady state

$$\int c(\delta\vec{E}\times\delta\vec{B})/4\pi\cdot dA = -\int \vec{F}_E\cdot d\Lambda$$

where the surface integral of the Poynting flux into a volume equals the surface integral of the kinetic energy flux out of the volume. The geometry of the surface integral is illustrated in Figure 1 which defines the surface of integration as a field-aligned surface which encloses a flux tube and two endcaps at 1 R_E and 5 R_E. In the absence of energy conversion ($J\cdot E = 0$), and neglecting any perpendicular Poynting flux flowing out of the flux tube, the Poynting flux flowing into the region at 5 R_E must equal the Poynting flux flowing out of the region at 1 R_E. Since the cross sectional areas of the end caps at 1 R_E and 5 R_E are inversely proportional to the background magnetic field strength, the Poynting flux scales proportionally with the magnetic field strength. In the presence of auroral particle acceleration, $J\cdot E > 0$, and a fraction of the incident Poynting flux is converted to particle energy flux. At small perpendicular wavelengths, electron inertial and kinetic effects give rise to a wave parallel electric field. In addition, parallel electric fields can arise due to nonlinear plasma effects such as double layers. Parallel electric fields can give rise to a small component of the wave Poynting flux directed perpendicular to the ambient magnetic field. This perpendicular component of the Poynting flux can direct energy into an inverted V structure where it is dissipated through particle acceleration (Mozer et al., 1980). We note that Figure 1 only illustrates the scenario for production of earthward electron beams and outflowing ions. In general (as is the case in our examples), electrons can also be accelerated upwards and ions downward. In addition, the figure, for simplicity, depicts the Poynting flux as associated with a time variable Alfven wave, but the Poynting flux could be associated with a steady state electric field structure with pairs of upward and downward field-aligned currents producing the magnetic field perturbation (as illustrated by *Mozer et al.*[1980]).

The weakest electron beams which can produce auroral emissions at the visual detection threshold have energy fluxes of ~1 erg/cm^{2}s at ionospheric altitudes. However, much stronger auroral beams have been observed. A recent statistical survey shows that the earthward energy flux in auroral electron beams in the premidnight local time sector at ionospheric altitudes exceeds 60 ergs cm^{-2} s^{-1} during 10% of spacecraft passes (*D. S. Evans, unpublished manuscript*, 1998) with maximum values up to 500 ergs cm^{-2} s^{-1}. The latitudinal scale size of intense energy flux was ~ 0.6° or less for 80% of Evans' events. Recent comparisons of FAST electron data at altitudes of 4000 km and airborne imagers showed that the difference in energy flux between the down going beams and upward secondary electrons peaked at magnitudes of about 25 ergs cm^{-2} s^{-1} when discrete auroral arcs occurred on conjugate magnetic field lines [*Stenbaek-Nielsen et al.*, 1998]. In addition, there is a lesser contribution to energy flux associated with ion beams and ion conics streaming away from the auroral acceleration region. These ion populations are energized in the auroral acceleration region by parallel electric fields (in the case of beams) and by transverse wave heating (in the case of conics). Outflowing ions are associated with energy fluxes of the order of 0.1 to 1 erg cm^{-2} s^{-1} [*Ghielmetti et al.*, 1979] or several percent of that found in the electron beams. Thus most of the particle energy flux generated in the auroral acceleration region resides in electron beams. For the purposes of this paper, it should be noted that the detection of upflowing ions during a pass through the plasma sheet is an important feature of our data set because it allows us to infer when the spacecraft is magnetically conjugate to the auroral acceleration region.

Over the large spatial scales encompassing the entire auroral zone, the energy flux dissipated in Joule heating of the

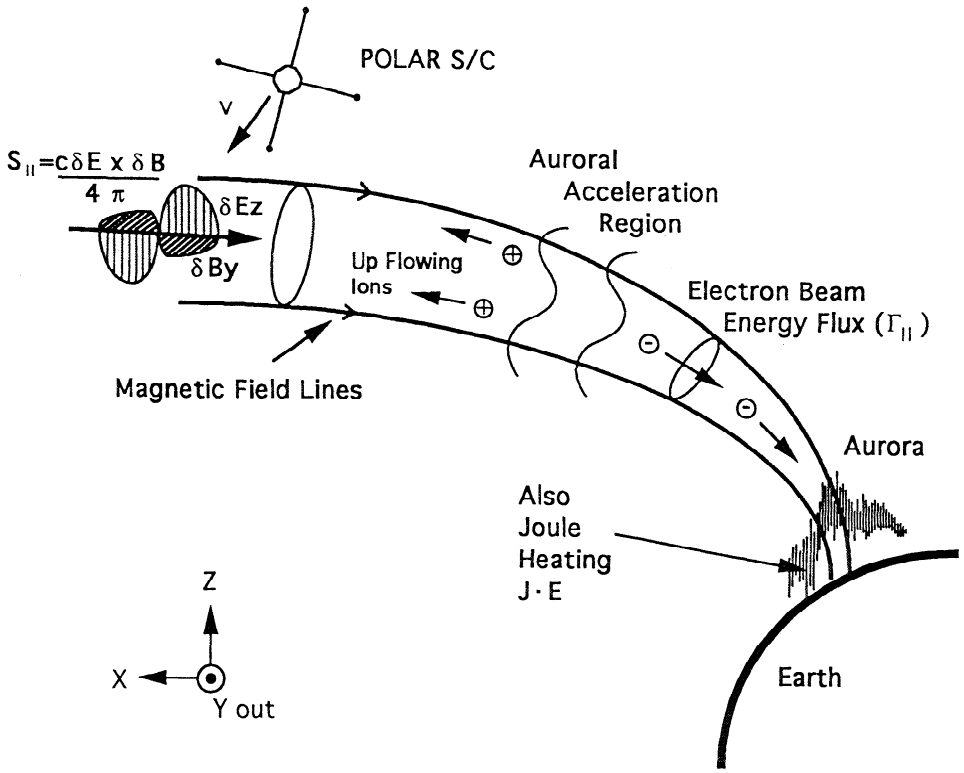

Figure 1. Illustration of a magnetic flux tube conjugate to the auroral acceleration region with incident Poynting flux and its conversion to energized particles and joule heating of the ionosphere. Wavelength of wave fluctuations not to scale.

conductive ionosphere due to the large spatial scale convection electric field and large-scale current systems is roughly 1-5 ergs cm^{-2} s^{-1} at ionospheric altitudes. On much smaller spatial scales at altitudes below 1800 kms, the Freja spacecraft has observed Poynting flux values of 1-10 ergs cm^{-2} s^{-1} [*Louarn et al.*, 1994] over spatial scales of about 1 km in association with kinetic Alfven waves. There have been estimates of Poynting flux of 0.1 to 4 ergs cm^{-2} s^{-1} at altitudes of 8000 km from the Akebono spacecraft [*Nagatsuma et al.*, 1996]. These lower-altitude observations consisted of roughly equal energy fluxes propagating toward and away from the Earth. Measurements of electron energy flux and Poynting flux using HILAT spacecraft data at altitudes of 400-1000 km, show that the Poynting flux ranged up to 6 ergs cm^{-2} s^{-1} over spatial scales of several degrees of invariant latitude [*Kelley et al.*, 1991]. Since these observations were obtained below the altitude of the auroral electron acceleration region, the measured Poynting flux provides an estimate of the energy flux dissipated in Joule heating of the ionosphere. Similar values of Poynting flux have been observed during sounding rocket flights above Sun-aligned polar cap arcs [*Kletzing et al.*, 1996]. The Poynting flux dissipated in the ionosphere may be regarded as the portion escaping through the lower "end cap" in Figure 1. The only previous measurements of Poynting flux at altitudes comparable to those of this study (> 4 R_E) were those obtained from the CRRES spacecraft near the inner edge of the plasma sheet (Maynard et al., 1996). During the onset of one intense substorm in that study, the net Poynting flux due to Alfven waves was directed toward the Earth along the ambient magnetic field and ranged up to 0.8 ergs $cm^{-2}s^{-1}$ for several minutes. This is similar to the observations presented here with the exception that our observations are near or at the outer boundary of the plasma sheet.

It should be noted that an important limitation of this study is that it is not possible to directly determine the surface integral of the Poynting flux at high altitudes since we do not know the velocity of the plasma sheet boundary past the spacecraft and cannot convert time domain data in the spacecraft frame to data which are a function of spatial coordinates. Thus the spatial scales of Poynting flux observed at high altitudes can not be determined and compared to the low-altitude latitudinal width of the electron energy flux in auroral beams. Similarly, the question of whether the structures observed herein are spatial structures or temporal structures awaits subsequent detailed analysis.

In summary, conservation of energy strongly suggests there should be processes operating above the auroral acceleration region which generate earthward directed Poynting flux which, when mapped along magnetic field lines to ionospheric altitudes, reaches 50 ergs cm^{-2} s^{-1} (or more) a significant fraction of the time. The actual Poynting flux measured at lower altitudes should be less since it is dissipated (primarily through the energization of auroral electrons) as it propagates toward the Earth. The Poynting flux should be strongly amplified in proportion to the magnetic field strength as it approaches the Earth, $S_1=S_2\,(B_1/B_2)$. At altitudes of 4-5 R_E near the plasma sheet boundary, the magnitude of the magnetic field is about 125 times less than at ionospheric altitudes. Therefore a Poynting flux of about 0.5 ergs cm^{-2} s^{-1} at 4-5 R_E above the auroral zone would account for strong auroral electron beams with energy fluxes of 50 ergs cm^{-2} s^{-1} at ionospheric altitudes.

2. Instrumentation

The electric field measurements on the Polar spacecraft are obtained from the U. C. Berkeley Electric Field Instrument [*Harvey et al.*, 1995]. The electric field is determined through measurement of the electric potential difference between pairs of current-biased spherical sensors. These sensors are deployed at the ends of three orthogonal pairs of booms with tip to tip separations 100 m and 130 m (in the spin plane) and 13.8 m (along the spin axis). The three-dimensional electric field vector is sampled at 20 samples/s. The magnetic field vector is sampled at 8.3 samples/s by the UCLA three dimensional fluxgate magnetometer [*Russell et al.*, 1995]. The Hydra particle detector [*Scudder et al.*, 1995] provides measurements of electron density and temperature, and electron and ion particle and energy flux with a 13.8 s time resolution. Images from the Ultraviolet Imager [*Torr et al.*, 1995] provide information on the spatial location of intense aurora and also an estimate of the energy flux of auroral electrons which caused the aurora. This instrument cycles through different filters in order to provide spectral information on the aurora. In this study, images were obtained using a filter centered on 1700 Angstroms with a band width of about 80 Angstroms which responds to molecular N_2 Lyman-Birge-Hopfield (LBH)-long wavelength emissions. These emissions are primarily due to electron impact excitation. This filter has been designed and calibrated to provide information on the total energy flux deposited by auroral electrons in the ionosphere and is accurate to about 50% [*Germany et al.* 1998]. The image has a spatial resolution of about 0.5° which is primarily due to a wobble in the spacecraft spin axis.

3. Plasma Sheet Pass on May 9, 1997

Plate 1 presents electric and magnetic field data and plasma measurements during an inbound pass from the tail lobe into the plasma sheet at a geocentric distance of about 4.5 R_E near 22 MLT on May 9, 1997, The electric and magnetic field data is averaged over 6 s. The plasma measurements are averaged over 13.8 s. During the hour encompassing this crossing, AE (preliminary) was ~100 nT to 150 nT. Plate 1 encompasses the time interval from 0530 UT to 0615 UT while the spacecraft moved from L=9.4 to 4.8. The top panel of Plate 1 shows the z GSE component of the electric field (northward and perpendicular to the ecliptic plane). The second panel displays the y component of the magnetic field with a Tsyganenko model magnetic field subtracted. This component is directed eastward in an azimuthal direction. The third panel displays the Poynting flux along the ambient average magnetic field. This component of the Poynting flux has been calculated from the three components of the perturbation electric field and three components of the perturbation magnetic field. These perturbation fields were calculated by detrending each component of the field by subtracting a 180 s running average from the original data. The Poynting flux vector calculated from these perturbation fields was then projected along the average magnetic field direction. The average magnetic field direction was calculated from the measured magnetic field vector averaged over 180 s. The fourth panel shows the sum of the electron and ion energy flux along the magnetic field (positive is downward) calculated from the Hydra measurements. The fifth panel shows the electron density. The sixth and seventh panels present color coded energy-time spectrograms of ion and electron energy fluxes. The vertical brackets in the top panel delineate time periods when the foot of the spacecraft magnetic field line mapped to within 1° of the regions of intense (>16 ergs cm^{-2} s^{-1}) auroral emission determined from the UVI images shown in Plate 2 (which will be discussed in the next section).

The particle data show that Polar entered the plasma sheet boundary layer from the lobe at 0537 UT at a geocentric distance of about 4.9 Re. The entry into the plasma sheet is most clearly indicated by the order of magnitude increases in the 2-20 keV electrons. The electric field enhancements are located on the high density side of a jump in density from very low values characteristic of the tail lobes (< 0.1 cm^{-3}) to 0.4 cm^{-3} on the plasma sheet side.

The electric field data show a series of three fluctuations ranging between -100 mV/m and 140 mV/m. The full width at half maximum of the center fluctuation is about 20 s. Cumulatively the three fluctuations last for about 300 s. This 5 min time interval coincides with the passage of the spacecraft through an upward current sheet as indicated by a shift in the dc level of By. Superimposed on this shift are three ~20 nT fluctuations in the magnetic field. These transverse magnetic field fluctuations are similar in wave form to those in the normal component of the electric field. The total magnitude of the magnetic field is about 400 nT. The variations in the total magnitude of the magnetic field, $\delta|B| = \delta (B_x^2+B_y^2+B_z^2)^{1/2}$ (not presented) are of the order of 1 nT over similar timescales during these waves. Thus the transverse variations in the magnetic field strongly dominate over the compressional variations as expected for Alfvenic fluctuations.

The net Poynting flux calculated from the detrended electric and magnetic fields consists of contributions from Alfven wave energy propagating toward and away from the Earth along the background magnetic field. The net Alfven wave power for this plasma sheet crossing is directed toward the Earth with amplitudes ranging up to 0.6 to 1 ergs cm^{-2} s^{-1}. The fact that the Poynting flux is directed toward the Earth indicates that the energy flux due to the Alfven waves propagating toward the Earth is larger than that from waves propagating away from the Earth. The existence of waves propagating away from the Earth can be deduced from the existence of phase differences between the electric and magnetic fields which will be discussed later. The scale on the right side of the Poynting flux plot of Plate 1 indicates the value of the Poynting flux as mapped to 100 kms altitude. The mapped Poynting flux ranges between 24 and 100 ergs cm^{-2} s^{-1} and is much larger than the Poynting flux previously measured in situ at lower altitudes in the auroral acceleration region. As previously discussed, this suggests that a significant portion of this energy flux is being dissipated through particle acceleration before it reaches the ionosphere.

Panels eight through thirteen of Plate 1 present electron and ion energy flux as a function of energy for pitch angles between 0° and 30°, 75° and 105°, and 150° to 180°. The data show that the electric field structures and earthward Poynting flux shown in panel 1 coincide almost exactly with 1-10 keV up-going ions which have been accelerated at lower altitudes in the acceleration region. These ions are labeled "UFI" in the bottom panel of Plate 1. They are located at the outer boundary of the plasma sheet and last for about 3 min. The values of the ion flux parallel (i.e., down-going) and perpendicular to the magnetic field are much less than the values of flowing away

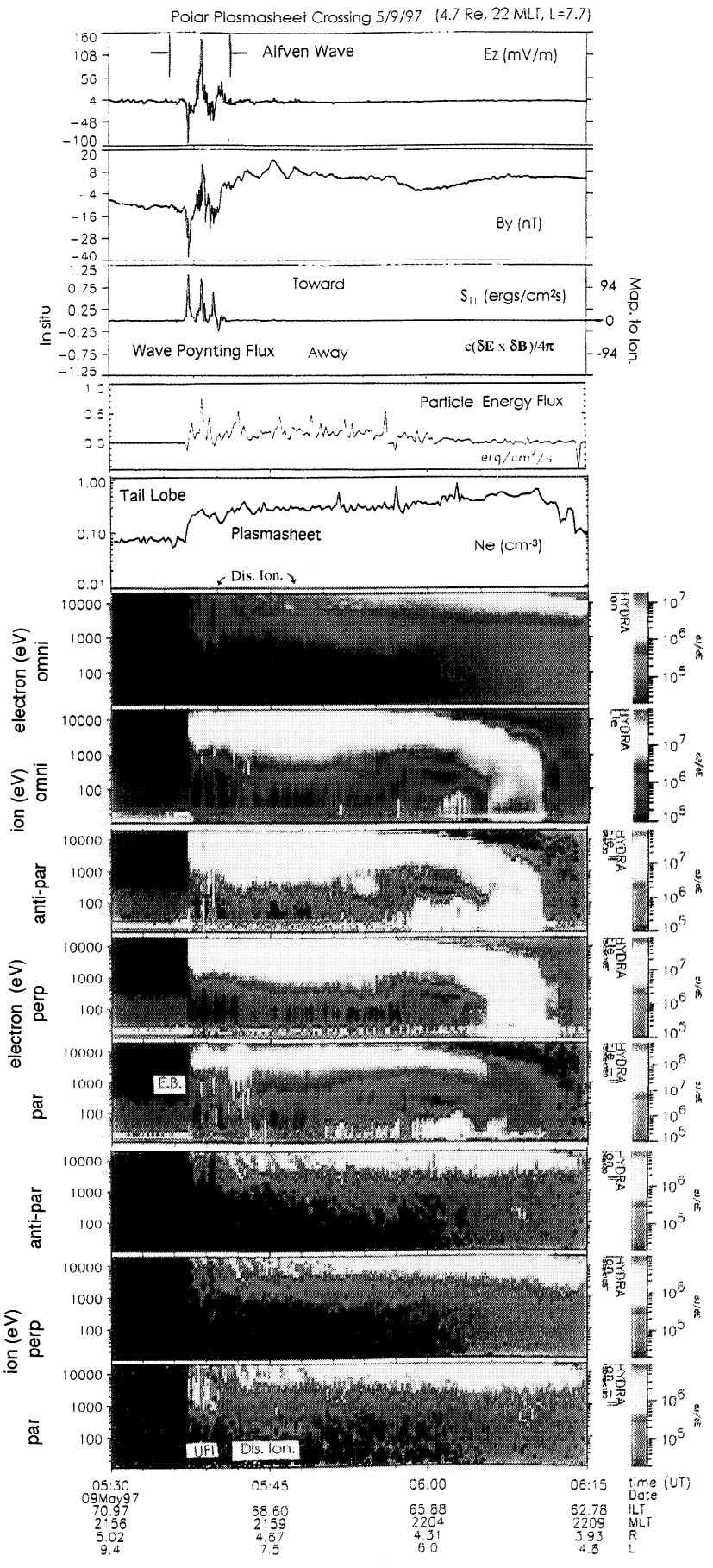

Plate 1. Measurements from Polar spacecraft crossing of the PSBL on May 9, 1997. The panels show (from top to bottom) the component of electric field approximately normal to the plane of the plasma sheet, the magnetic field component (model subtracted) perpendicular to the local magnetic field in the plane of the plasma sheet towards the East. The third panel presents the component of the Poynting flux along the magnetic field (towards the Earth). The fourth panel is the total particle energy flux along the magnetic field with positive values corresponding to earthward flux. The fifth panel is the electron density obtained from the Hydra measurements. The sixth and seventh panels display Hydra energy flux-time spectrograms of electrons and ions. The eighth and ninth panels present Hydra electron energy fluxes along look directions which are, in sequence, parallel (toward the Earth), perpendicular, and anti-parallel to the magnetic field vector. The final three panels show ion energy fluxes parallel, perpendicular, and anti-parallel to magnetic field.

from the Northern Hemisphere and indicate the ions are streaming away from the Northern Hemisphere along the magnetic field. A more detailed analysis of the data indicates that these ions are almost completely field-aligned. As discussed in the Introduction, the beams provide evidence that the Polar spacecraft is magnetically conjugate to the auroral acceleration region. There is also evidence for intermittant ~ 1 keV field-aligned electron beams traveling both toward and away from the Northern Hemisphere's ionosphere. The electron beams may be found in the eighth and tenth panels of Plate 1 and occur immediately following the label "E.B" in panel ten. The electron fluxes streaming into the Northern Hemisphere (panel eight) coincide in time very closely with the period of the upflowing ions and the layer of earthward Poynting flux. The outward flowing electron fluxes occur over a broader time scale. These beams are further evidence that during the time intervals of strong earthward Poynting flux, Polar is on field lines associated with the Northern Hemisphere auroral acceleration region. Upflowing electron beams are a common observation at lower altitudes in downward current regions in the auroral acceleration region [*Carlson et. al.*, 1998]. The beams accelerated along the magnetic field toward the Northern Hemisphere ionosphere could have originated in the Southern Hemisphere. Alternatively, they could have been generated by acceleration structures near the spacecraft or at altitudes above the spacecraft on the same magnetic field line. Finally, they could have been generated in the Northern Hemisphere, accelerated away from the earth, and magnetically mirrored in the Southern Hemisphere.

As the spacecraft moves deeper into the plasma sheet, it leaves the layer of strong Poynting flux and electric fields and the ion data shows a sequence of nested signatures of 2 to >20 keV energy dispersed ions (labeled "Dis. Ion" in the bottom panel) bouncing between opposite hemispheres. This is indicated by the fact that the nested traces, when carefully inspected, alternate between the 0°-30° pitch angle plots and the 150°-180° pitch angle plots. Field-aligned ion fluxes both parallel and anti-parallel to the magnetic field over energy ranges from tens of electron volts to 45 keV are a crucial signature of the boundary layer as defined by *Williams et al.* [1982], *Eastman et al.* [1984], and *Fairfield* [1987]. The inner edge of the plasma sheet is encountered at about 0606- 0612 UT, where the electron energy begins to drop to plasmaspheric values.

The particle energy flux shown in panel four of Plate 1 maximizes near the outer edge of the plasma sheet at values of 0.8 ergs cm^{-2} s^{-1}. This peak coincides with the peak in Poynting flux. Although only the total energy flux is plotted in panel 4 of Plate 1, an inspection of the ion and electron contributions shows the electron contribution dominates over the ion by 1-2 orders of magnitude.

The correlated electric and magnetic field spikes in panels one and two of Plate 1 are consistent with the propagation of incident and reflected Alfven surface waves or pulses along the magnetic field as we shall show below. The surface "waves" are confined to a thin layer along the plasma sheet boundary near the plasma sheet/tail lobe density jump. The ratio of $\delta E_z/\delta B_y$~ 4000 to 10000 km/s calculated from the peak values of the fields coincides with a reasonable estimate of the Alfven speed in this region. This value of the ratio of the electric to magnetic field variations is 1-2 orders of magnitude larger than the ratio expected for steady state structures associated with field-aligned currents closing through the ionosphere in the absence of magnetic field-aligned electric fields. In that case, $\delta E/\delta B=c/\Sigma_p$, where c is the speed of light and Σ_p is the height integrated Pedersen conductivity which should be 5-10 mhos in an area of active auroral electron precipitation .

The value of large-scale convection electric field in the plasma sheet as displayed in panel one of Plate 1 is much smaller than the electric field associated with the Alfven wave structure. Close inspection of the electric field data with at a finer vertical resolution than available in Plate 1 shows that, at locations displaced from the effects of the large-amplitude Alfven wave, it is of the order of 1 mV/m. At the location of the Alfven wave, (which has amplitudes exceeding 100 mV/m), the inferred value of the average convection electric field can only be determined by averaging over the Alfven wave. As might be expected, the value obtained from the averaging of the large-amplitude Alfven wave depends sensitively on time scales over which the data are smoothed. The value of large-scale electric field is therefore uncertain at the position of the Alfven wave. We estimate an upper bound on the large-scale electric field of about 4 mV/m. The magnetic field perturbation associated with the large-scale field-aligned current system was about 25 nT. The Poynting flux estimated from these fields is of the order of about 0.01 to 0.04 ergs cm^{-2} s^{-1} near the Alfven wave and about 0.01 ergs cm^{-2} s^{-1} away from the Alfven wave. If these values are mapped to 100 km altitude, the Poynting flux ranges between 1-4 ergs cm^{-2} s^{-1} at the conjugate position of the Alfven wave and 1 erg/cm^2s else where. Note that this is roughly comparable to the values of Poynting flux (6 ergs cm^{-2} s^{-1}) measured by Kelley et al., (1991) at low altitudes associated with Joule heating of the ionosphere. The conclusion, which is comparatively insensitive to the errors inherent in this analysis, is that the Poynting flux due to the Alfvenic structures we have presented herein is 1-2 orders of magnitude more intense than the Poynting flux due to the larger spatial scale field-aligned currents and convection electric fields which map electrostatically to the ionosphere.

Figures 2a and 2b present an expanded view of about 8 min of data from Plate 1 encompassing the interval of strong electric fields. Figure 2a includes measurements of Poynting flux, Ez and By at a 0.5 s time resolution. There is a phase lag between the electric and magnetic field signals with the electric field spikes maximizing on the leading edge of the magnetic field signals. This is consistent with interference between the incident and reflected pulse. A wave which has reflected off a conducting ionosphere has a reversed tangential electric field component and a magnetic field component in the same direction. Thus after the reflected wave arrives at the spacecraft, there is destructive interference between the electric field pulses and constructive interference for the magnetic field pulses. As noted previously, despite the existence of the reflected wave, the measured Poynting flux shows that the total observed electromagnetic energy flow is strongly earthward during this event.

Figure 2b presents the full vector electric field at a 0.5 s time resolution in a magnetic-field-aligned coordinate system. (This is the only figure for which this coordinate system is used). The z_FAC direction points along the three minute average of the ambient magnetic field **B**. The y_FAC direction is directed along $\mathbf{B}\times\mathbf{R}_{SC}$, where $\mathbf{R}_{SC}$ is the spacecraft position

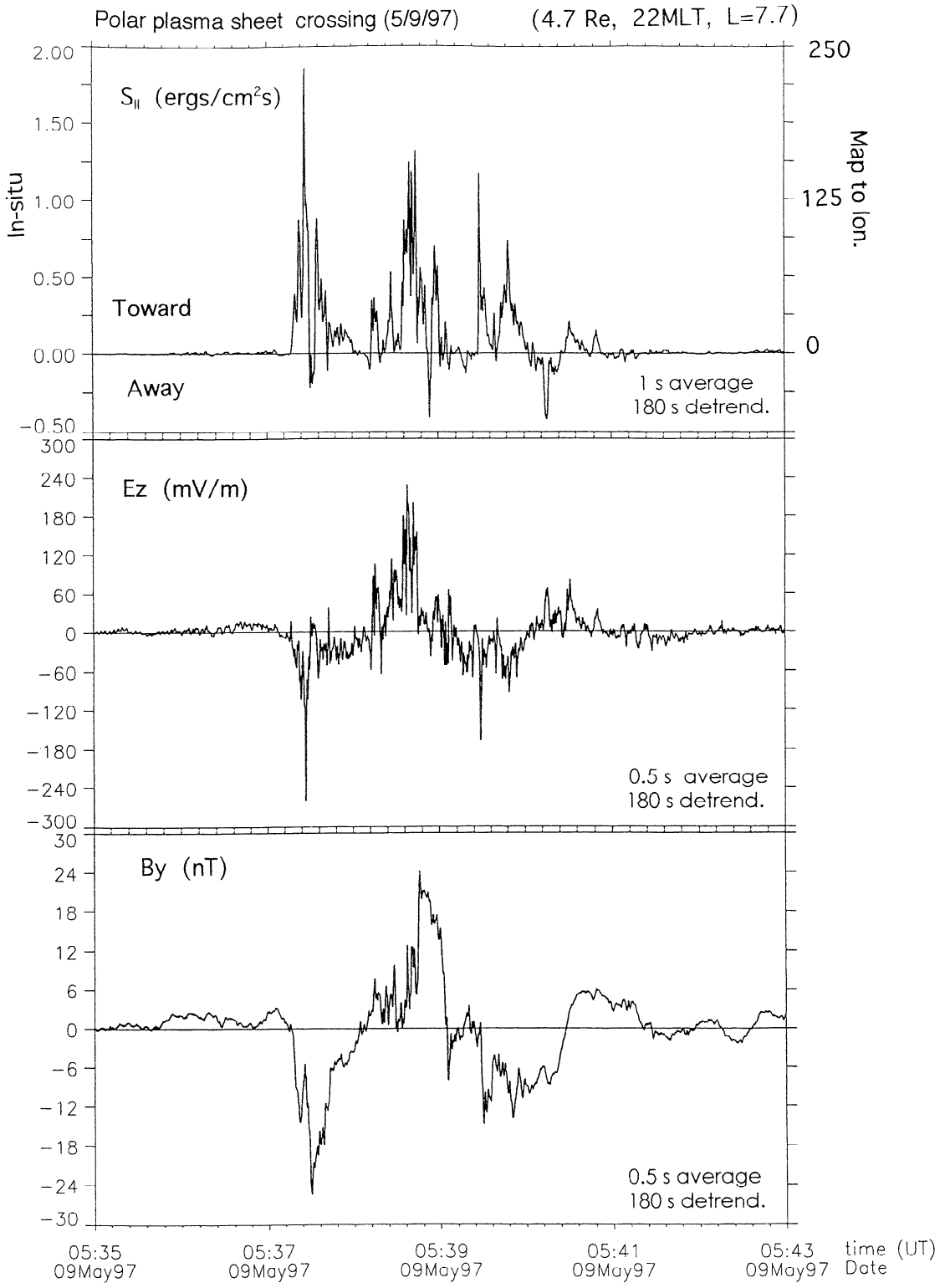

Figure 2a. Expanded view of the Poynting flux, Ez, and By from May 9, 1997 during the interval of large electric fields from Plate 1.

vector relative to the center of the Earth. The *x*_FAC direction completes the right-handed coordinate system. Since the measured total magnetic field vector is directed approximately toward the Sun, the *z*_FAC direction nearly points toward the Sun, the *y*_FAC direction is eastward, and *x*_FAC direction is normal to the ecliptic and southward. Notice that Ex_FAC is inverted relative to the Ez component displayed in Plate 1 Figure 2a, and Plate 2 of this paper. Figure 2b shows that the electric field in the *x*_FAC direction (or in the direction normal to the ecliptic) is larger by factors of 2 or 3 than the other components. Using the simplest assumption of the average spatial configuration of the plasma sheet, we conclude

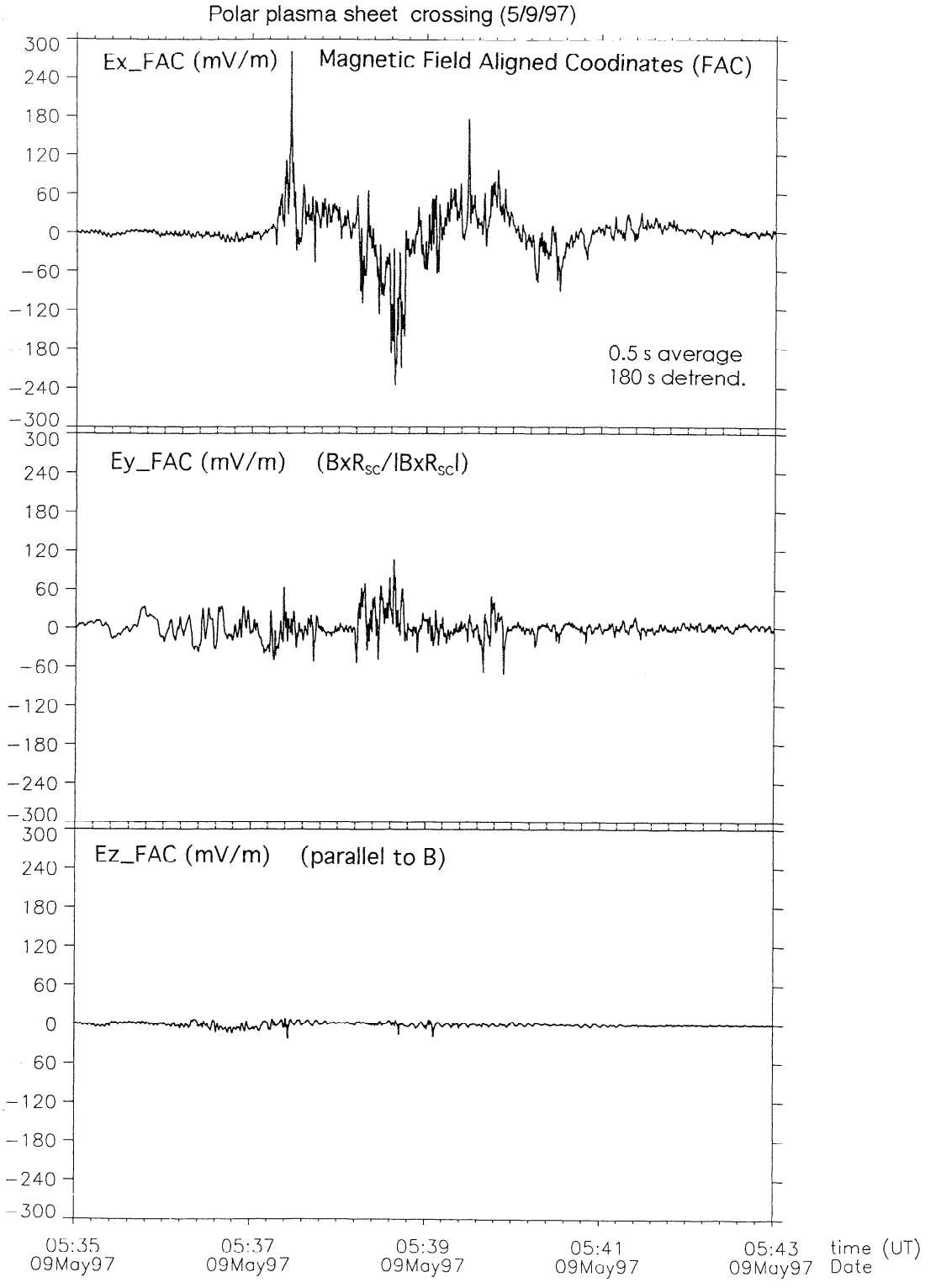

Figure 2b. Expanded view of three components of the electric field data from May 9, 1997, as presented in a magnetic field-aligned coordinate system.

that the x_FAC direction points roughly along the average plasma sheet normal. This is the direction one would infer for the average plasma sheet normal on the basis of simple symmetry and also on the basis of the statistical spatial distribution of plasma sheet plasma at higher altitudes [see, e.g., *Fairfield,* 1987, Figure 6]. We infer from this that the electric field has a very strong component normal to the plasma sheet boundary (Ex_FAC) as compared to tangential to the boundary (Ey_FAC). We note that this conclusion is relatively insensitive to errors (20°-30°) in the actual direction of the plasma sheet normal. This component of the electric field is not typically measured by spacecraft in the tail

(ISEE-1) and it is typically the component which is the largest in the Polar data set and which is associated with most of the Poynting flux energy transfer.

Figure 2b also shows that the component of the electric field parallel to the average magnetic field is 2 orders of magnitude smaller than the perpendicular component of the electric field. The residual electric field in the parallel direction should not necessarily be interpreted as a accurate indication of component of the electric field parallel to the magnetic field since the coordinate system is constructed from three minute averages of the magnetic field and the instantaneous magnetic field direction varies from the average direction due to large-amplitude Alfven waves. We further note for completeness that the electric field in the *y*_FAC direction is measured primarily by the 13.8 m spin axis booms and is not as accurate as Ex_FAC and Ez_FAC which are measured by the >100 m spin plane booms. However, the large-amplitude electric fields which we are investigating here are much larger than error contributions to the measurement.

4. UVI Images During the Plasma Sheet Crossing on May 9, 1997

Plate 2 presents a sequence of eight UVI images using the LBH-long filters taken during a 10 min interval encompassing the strong electric fields and Alfven waves of Plate 1. The images start at 0535 UT and end at 0544:31 UT. The time of each image is displayed above each image. Images using the LBH-long filters are interwoven with images using other filters (not shown) and are obtained at time intervals alternating between 19 s and 165 s. The images are color-coded in photon flux and the conversion to energy flux is shown in the final image. The images show that throughout this 10 min period there was an auroral arc centered at ~69° invariant latitude at ~2130 MLT. The region of strongest emission is red with a white center. The scale indicates that these intensities are typically associated with an energy flux of auroral electrons ranging from 20 ergs cm^{-2} s^{-1} to above 27 ergs cm^{-2} s^{-1}. The arc is nearly constant in intensity and position over this time interval; however, a close inspection indicates that it is moving slightly westward and northward and is slowly fading in intensity over the time interval of the pass. The mapped foot of the Polar magnetic field line is denoted by a small (faint) cross. The estimated accuracy of this mapping is about 1°. The spacecraft remains in the vicinity (~ 1°) of the brightest region over a period of 5-10 min. It is clear that the large-amplitude electric fields and the associated strong Poynting flux are observed on this pass only during time periods when the spacecraft is nearly magnetically conjugate to the brightest auroral emission features. During such times, the electric fields and Poynting flux vary on time scales and spatial scales which can not be resolved by the images. The peak values of the Poynting flux range up to factors of 3 larger than the energy flux due to precipitating electrons as estimated by the imager. The mapped Poynting flux is about 100 ergs cm^{-2} s^{-1}, while the energy flux associated with the region of bright auroral emission is typically 20 ergs cm^{-2} s^{-1} in the region conjugate to the spacecraft position. As previously discussed, the incident Poynting flux must account not only for the energy flux of precipitating electrons, but also for significant contributions from ionospheric Joule heating, and lesser contributions from ion acceleration. In addition, the spatial/temporal scales over which the Poynting flux varies are much smaller than those resolved by the images. The images average over ionospheric spatial scales of about 0.5°. This is much larger than the 0.1 to 50 km spatial scales of discrete auroral arcs. In addition, an inspection of low-altitude FAST data shows that the latitudinal extent of localized electric fields may be an order of magnitude smaller than the latitudinal extent of the electron beams [*Ergun et. al.*, 1998]. Under these circumstances, the peak value of the Poynting flux measured by the higher-resolution satellite measurements should be an order of magnitude larger than the value of the electron energy flux inferred from the averaged images. Nevertheless, the comparison of the Poynting flux measurements at high altitude to the UVI images suggests that the Poynting flux is in part being converted to particle energy in the acceleration region, probably in association with the several hundred mV/m to 1 V/m localized electric field structures first observed by the S3-3 spacecraft over 20 years ago and now resolved routinely by the Polar and FAST spacecraft.

5. Plasma Sheet Crossing on May 1, 1997

In contrast to the May 9, 1997 event, the pass of May 1, 1997 shown in Plate 3, occurred when the aurora were highly variable and magnetic activity was much stronger than the previous event (Kp=5+, AE=1000 to 1500 nT). The data in Plate 3 are presented in the same format as the first seven panels of Plate 1 with the same time resolution and averaging. The first encounter with the plasma sheet occurred about 30 min prior to the beginning of Plate 3. The beginning of Plate 3 coincides with an interval when >1 keV ions and electron fluxes were strongly diminished. At about 2025 UT the Polar spacecraft encountered enhanced electron and ion fluxes over energies between 1 and 10 keV. These flux increases were coincident with a >50 nT decrease in By. This is consistent with the presence of plasma sheet fluxes and an encounter with the region 1 current system. Superimposed on this DC shift are fluctuations in By over periods of roughly 5 min. These fluctuations suggest slow temporal and or spatial variations in the large-scale field-aligned current system. The electric field fluctuations also increase from very small values in the tail lobes (< 1 mV/m) to between 5mV/m and 100 mV/m in concert with this entry into the plasma sheet. The enhanced fluctuation level suggests observations of the high altitude mapping of turbulent auroral electric fields. Within this region of electric field turbulence, the electric field is typically 5-10 mV/m with brief intervals of very strong localized electric fields ranging in amplitude between 10 and 80 mV/m. Notice that, unlike the May 9, 1997 event, there is no associated density jump. We focus on a brief episode of electric fields at about 2028 UT with a peak value of about -80 mV/m. This interval is associated with an enhancement in the Poynting flux ranging between 0.3 and 1 erg/cm^2s along the magnetic field and toward the Earth. When mapped to the ionosphere, this Poynting flux supplies peak energy fluxes of about 38-125 ergs cm^{-2} s^{-1} averaged over the 6 s time resolution of the data. In this pass, as in the pass on May 9, the Poynting flux associated with what appears to be slowly varying magnetic field variations indicative of large-scale quasi steady state field-aligned currents is much smaller in amplitude than the Poynting flux associated with variations on faster spatial/temporal scales.

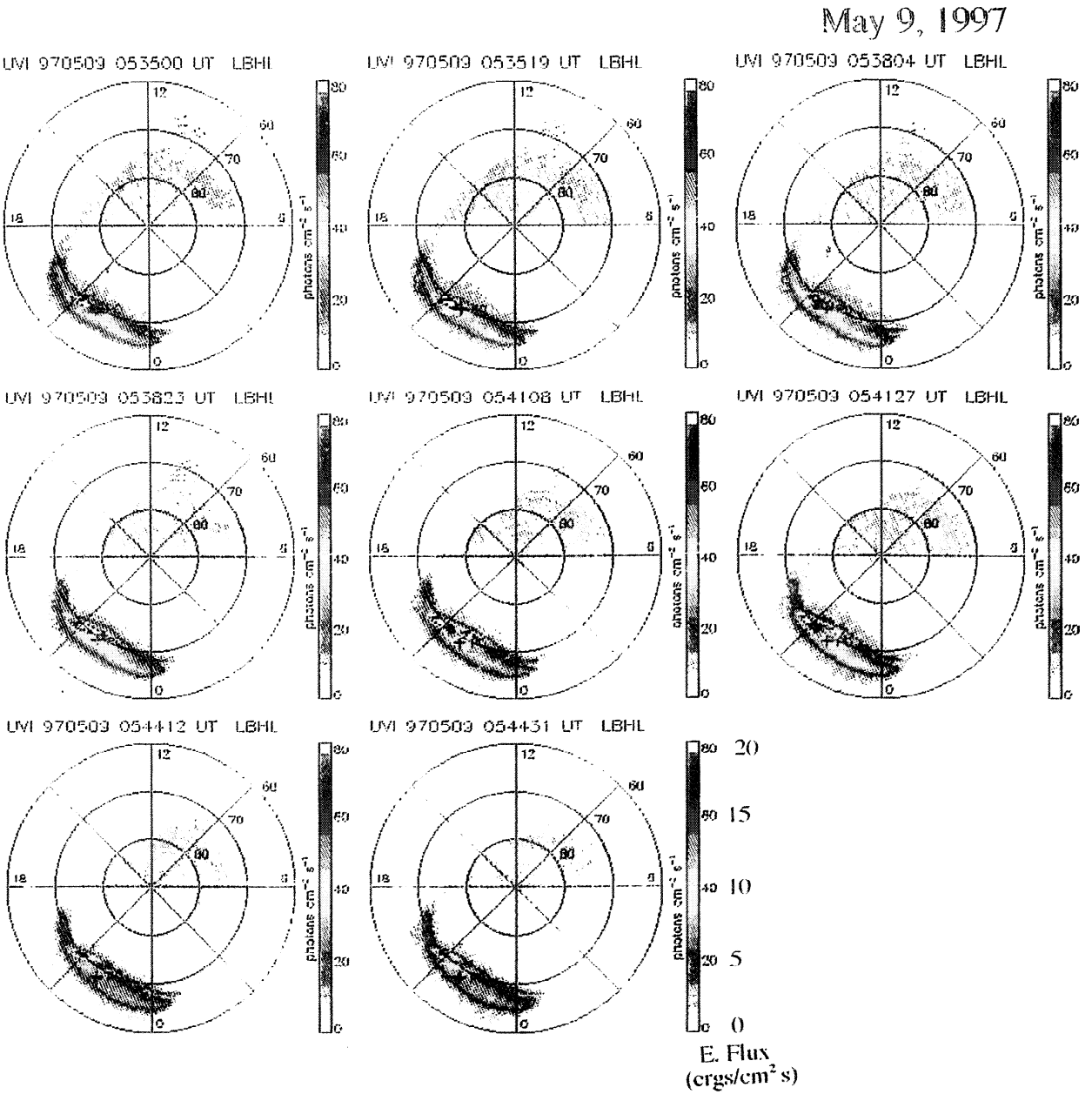

Plate 2. Images of the aurora from the UVI instrument on the POLAR spacecraft on May 9, 1997. The LBH-long filter used in this image provides an indicator of the total energy deposited in the ionosphere by auroral electrons. The track of the spacecraft is indicated by the small cross (+).

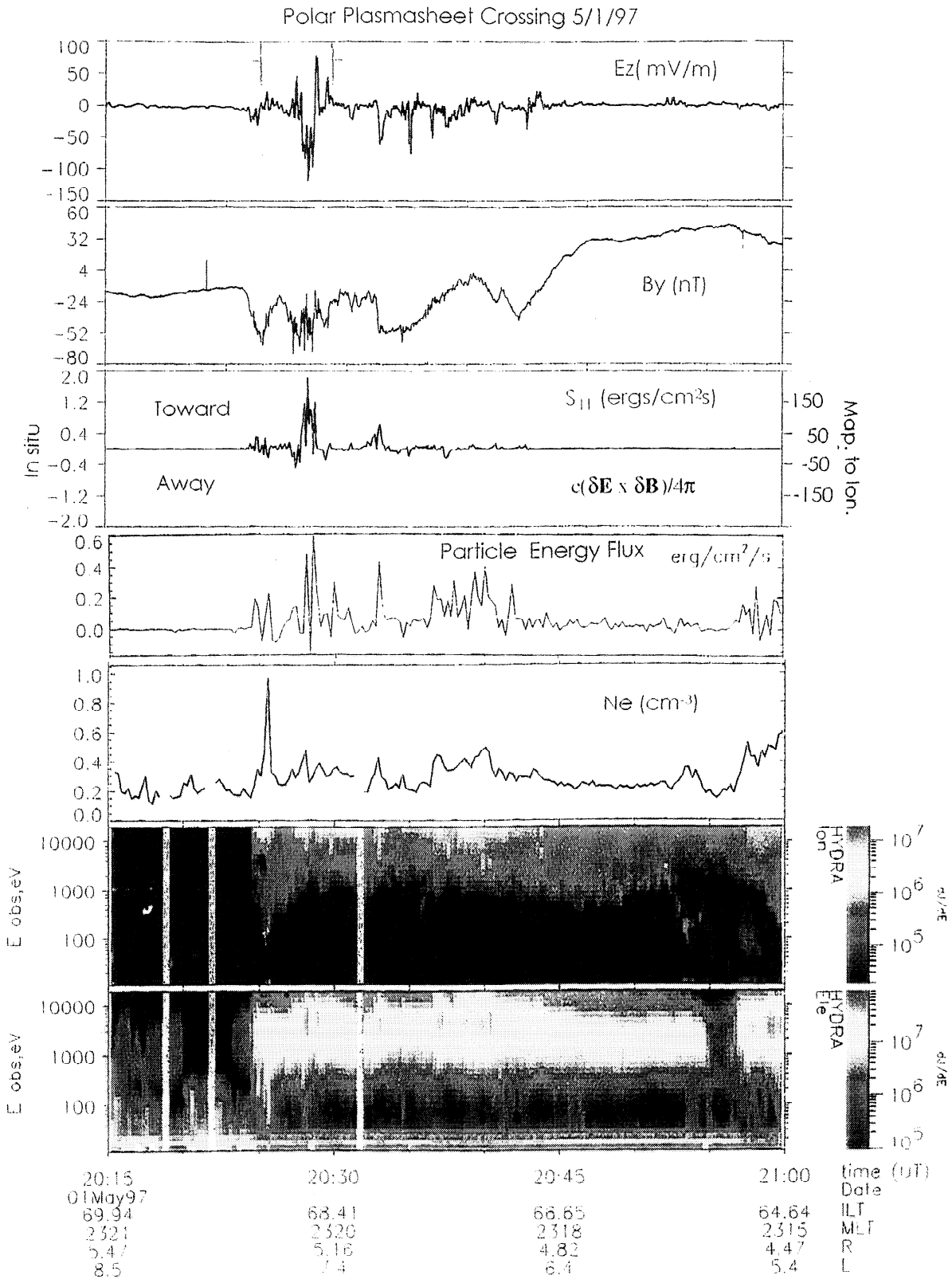

Plate 3. Data for the lobe-PSBL crossing on May 1, 1997. The panels are in the same format as in the first seven panels of Plate 1.

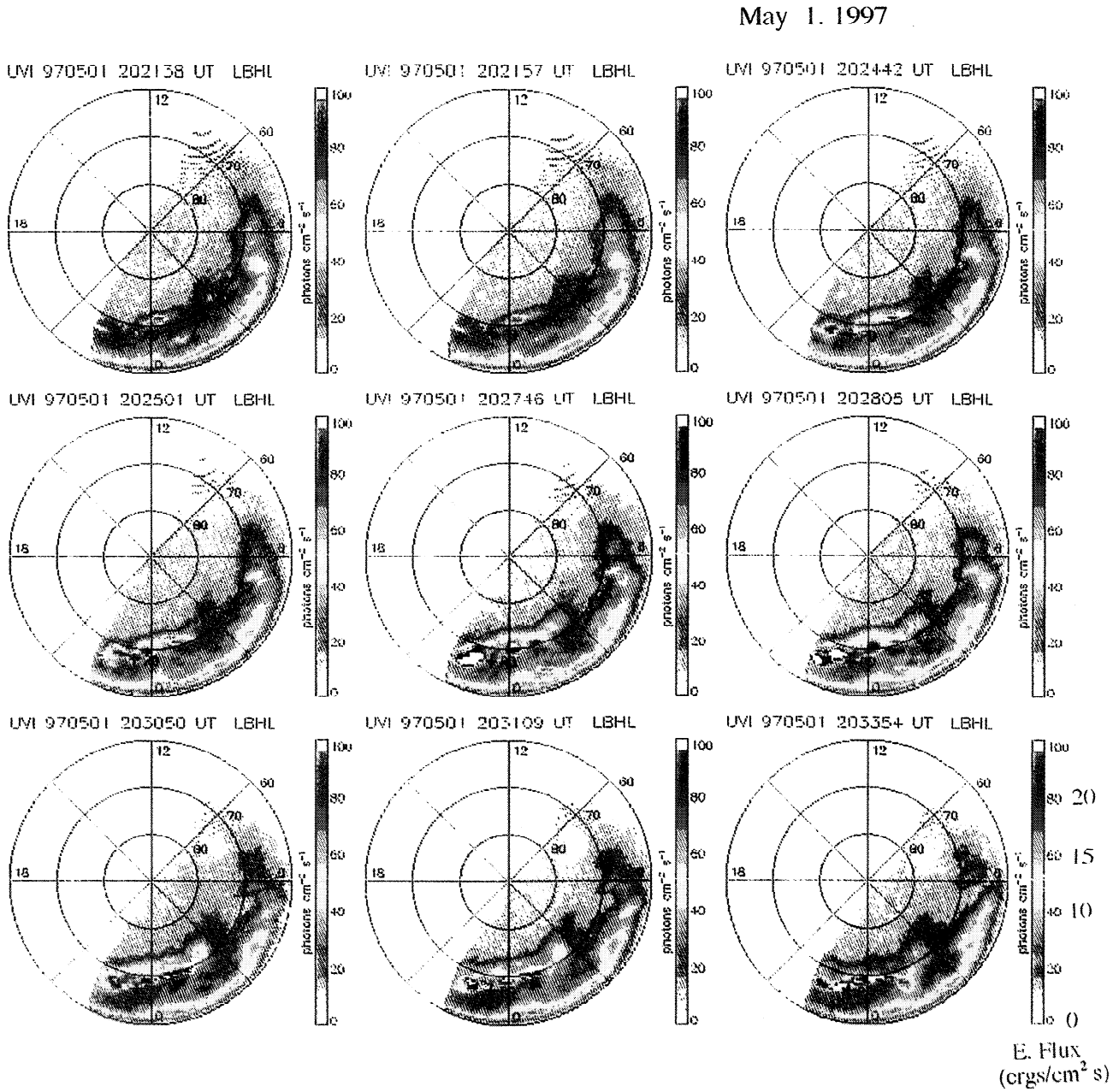

Plate 4. Images of the aurora from the UVI instrument on the POLAR spacecraft on May 1, 1997. The LBH-long filter used in this image provides an indicator of the total energy deposited in the ionosphere by auroral electrons. The track of the spacecraft is indicated by the small cross (+).

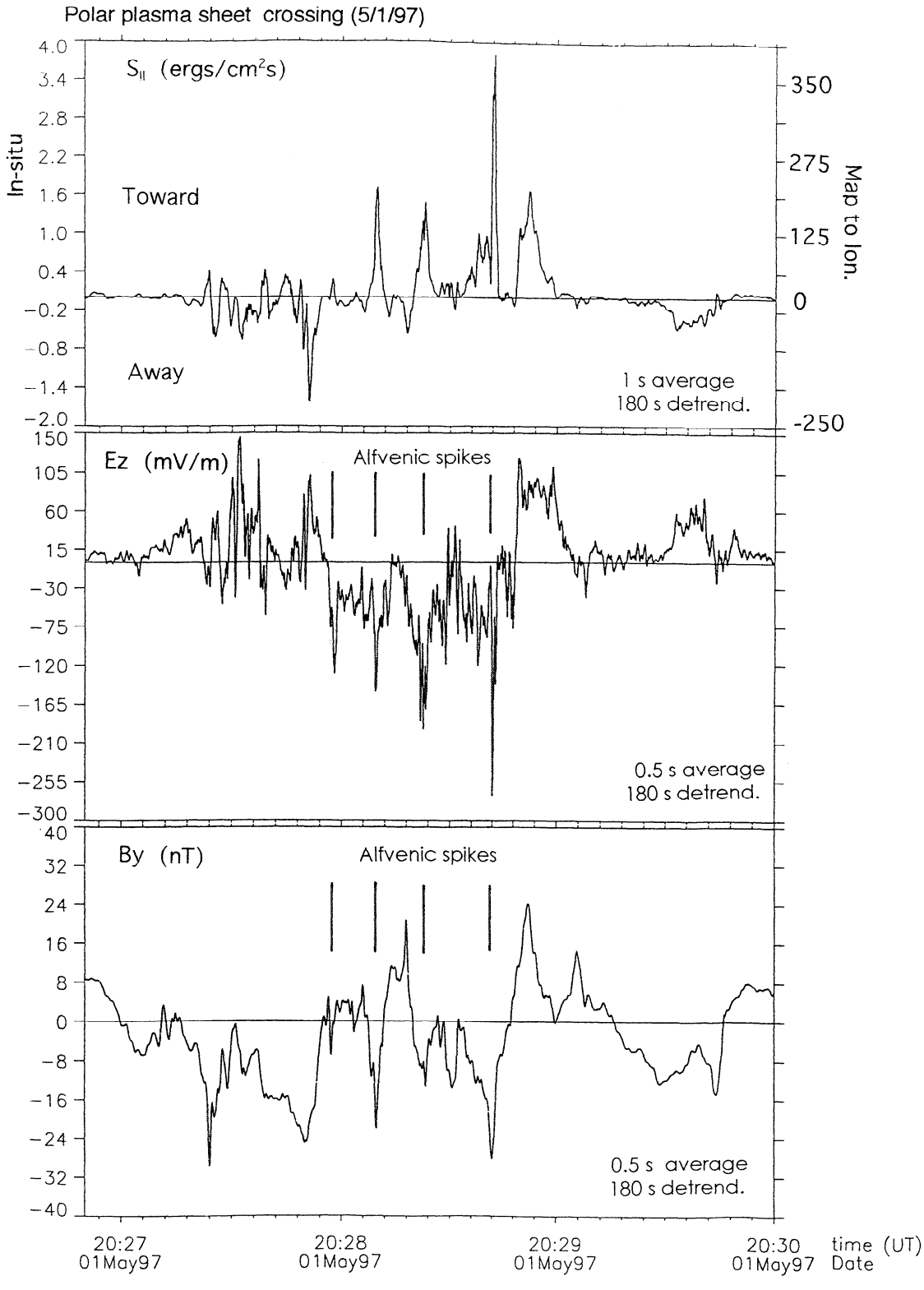

Figure 3. An expanded view of the Poynting flux, Ez, and By from May 1, 1997, during the large electric field event shown in Plate 3.

Figure 3 presents 0.5 s time resolution data over the time interval from 2026:40 UT to 2030:00 UT encompassing the large Poynting flux and spiky electric and magnetic fields observations of the previous figure. The data reveal a sequence of electric field spikes with time durations of 1-3 s and amplitudes up to 200 mV/m. The electric field spikes are in phase with magnetic spikes of about 30 nT. The magnitude of the magnetic field is about 400 nT. The perturbations in the magnitude of the total magnetic field are of the order of three nT or less indicating the spikes are largely magnetically incompressible fluctuations as expected for Alfven waves. The E/B ratio is in the range of 3000-7000 km/s. An

inspection of the full vector electric field measurements (not included here) shows that the z component which points nearly perpendicular to the ecliptic and northward dominates over the other two components of the electric field. As discussed previously, this suggests that the component of the electric field normal to the plasma sheet is the dominant component. The large value of E/B, its similarity to estimates of the Alfven velocity (based on the measured density and magnetic field magnitude), and the orientation of the electric and magnetic field vectors suggest that the structures are propagating Alfvenic waves.

The magnitude of the Poynting flux along the magnetic field has been calculated and is ~ 3.8 ergs cm^{-2} s^{-1} for the largest spike. This value of the Poynting flux mapped to the ionosphere would be about 400 ergs cm^{-2} s^{-1}.

6. UVI Images for Plasma Sheet Crossing on May 1, 1997

Plate 4 presents a sequence of UVI images which indicate that, in contrast to the May 9, 1997, data, the aurora is strongly structured on large spatial scales and extends over a wider latitudinal scale. There are two latitudinally confined bands of strong emissions, one centered at about 70° and another at about 62°. The mapped position of the spacecraft slowly moves southward from 69° to 67° invariant latitude at about 2330 MLT. Over the period of the first six images from 2021 UT to 2028 UT, there is a strong enhancement in the spatial extent and intensity of the emission in the latitudinally confined auroral structure near the spacecraft conjugate point. The energy flux of auroral electrons within 1° of the spacecraft conjugate point increases by about a factor of 5 from about 5 ergs cm^{-2} s^{-1} to > 25 ergs cm^{-2} s^{-1}. A close inspection of the sequence of UVI images shows that, near the spacecraft footpoint, there are a number of intervals of auroral intensifications and fading throughout the period from 2021 UT to 2034 UT. The strongest intensifications near the foot of the spacecraft magnetic field line occur during the images at 2027:46 and 2028:05 UT. The localized regions which are colored "white" in the image exceed 27 ergs cm^{-2} s^{-1} which is the saturation level of the color-coded scale. An inspection of images with a higher value for the saturation of the color scale shows that this region of intense auroral emission was associated with an energy deposition rate of 40-50 ergs cm^{-2} s^{-1}. The next image in the UVI sequence occurs 2 min and 45 s later at 20:30:50. Plate 3 shows that the time of the strongest Poynting flux as observed by the Polar spacecraft occurs between 2028 to 2029 UT. This period also corresponds to the interval of ~1 s Alfvenic spikes displayed in Figure 3. Although the time resolution of UVI is slower than that of the electric field instrument, within the time resolution of the 19-165 s spacing between successive UVI images, the period of the strong Poynting flux at Polar altitudes corresponds to the period of the strongest energy flux in the UVI images at or near (~1°) the foot of the Polar field line. Differences between the Poynting flux measurements may in part be a consequence of the fact that the Poynting flux (and also the aurora) varies on spatial and/or temporal scales much smaller than the UVI images can resolve. In addition, there are uncertainties in mapping of the magnetic field line from Polar to 100 km altitude which for different magnetic field models are of the order of 1°.

7. Discussion of Spatial and Temporal Scales (Ambiguities and Implications)

In interpreting the observations presented herein, it should be noted that the unknown velocity of the plasma sheet boundary relative to the spacecraft produces ambiguities in the temporal and spatial scales observed by the spacecraft. In this section we discuss the possible spatial and temporal scales for the different structures discussed in this paper and some of the implications of these scale sizes. In general, the temporal structures, as observed in the spacecraft frame, are Doppler shifted by $T_{SC} = T_{PS} + L_{\perp}/(\mathbf{V}_{PS}-\mathbf{V}_{SC})\cdot\mathbf{n}$, where T_{SC} is the duration of the structure seen in the spacecraft frame, T_{PS} is the duration as seen in the rest frame of the plasma sheet, $\mathbf{V}_{SC}$ is the velocity of the spacecraft relative to an Earth fixed frame, $\mathbf{V}_{ps}$ is the velocity of the plasma sheet boundary in the same frame, $\mathbf{n}$ is the unit vector normal to the plasma sheet, and $L_{\perp}$ is the scale size of the electric field structure in the direction perpendicular to the plasma sheet.

As shown in Plate 1 and Figure 2a, the strong electric and magnetic fluctuations observed during the May 9 plasma sheet crossing result in a layer of strong electromagnetic energy flow which begins at the plasma sheet density jump and continues for about 150 s as the spacecraft moves deeper into the plasma sheet. In the absence of direct measurements, we offer the following indirect arguments which provide rough bounds on the plasma sheet velocity relative to the spacecraft and on the spatial scale for this layer. A lower bound on this velocity is the velocity of the spacecraft itself due to its Keplerian orbit. This velocity is about 4 km/s. A second estimate is derived from measurements of the poleward velocity of auroral arcs during the expansion phase of substorms. Measurements by *Kelley et al.* [1971] indicate that this velocity is of the order of 1-2 km/s. If we assume the motion of the arcs is caused by expansion of the plasma sheet, the divergence of magnetic field lines in the dipole approximation implies the velocity should be about 10-20 km/s at Polar altitudes. The final estimate relies on arguments concerning mapping of the typical thickness of field-aligned current sheets. The width of the region 1 current system in the premidnight sector is typically about 3° in invariant latitude or ~300 km at 100 km altitude. Using a dipole mapping (which should be accurate for these altitudes), the typical field-aligned current structure maps to a spatial scale about 10 times as wide or about 3000 km at the altitude of the spacecraft. We compare this spatial scale to the actual observations of the region 1 current sheet in Plate 1 on the May 9 plasma sheet crossing. The dc shift in By, identified as the high-altitude mapping of the region 1 current structure, should have a width of about 3000 km. In the plot the change in By (the width of the current sheet) lasts for about 300 s so the plasma sheet boundary must be moving past the spacecraft at about 10 km/s (which is much larger than the velocity of the spacecraft. On the basis of these three arguments a very rough estimate of the plasma sheet velocity relative to the spacecraft, resting on these indirect arguments, is between 4 km/s and 20 km/s.

If the large-scale electric field structures are nearly time stationary in the frame of the plasma sheet and simply carried over the spacecraft by the motion of the plasma sheet, the spatial scale in the direction normal to the plasma sheet of the region of space encompassed by the brackets in the upper panel of Plate 1 (beginning at 0537 UT) which lasts about 360

s is 360 s x 4-20 km/s or ~1500 to 7000 km. This layer contains the three strong impulsive enhancements of electromagnetic flux lasting about 20 s and also encompasses the region of strong magnetic-field-aligned electron beams and outflowing ions. If mapped back down to ionospheric altitudes, this 360 s time interval has a latitudinal spatial scale of about 150-700 km at 100 km altitude. This range of spatial scales encompasses scale sizes between that of the brightest features resolved in the UVI images (which have scale sizes of about 1°) to the scale sizes of the entire region of auroral emission in the image which is ~5°.

The 20 s duration of the Poynting flux enhancements could either be temporal or spatial. If the Poynting flux variability is the consequence of a spatial structure convected over the spacecraft, its scale size is 20 s x 4-20 km/s ~ 80 to 400 km. Mapped to 100 km altitude, the scale size of the Poynting flux layers would be 8 to 40 km. Alternatively, in the limit that the Poynting flux enhancements are purely temporal, the observed variations in Poynting flux could be due to the occurrence of three 20 s impulsive bursts of Poynting flux during a time interval of 360 s. Under this circumstance the perpendicular spatial extent of the Poynting flux could range over the large-distance scales (1500 to 7000 kms) discussed above.

The high time resolution data in Figures 2a and 2b show the electric fields, magnetic fields, and Poynting flux are highly structured with fluctuations occurring on time scales in the spacecraft frame ranging down to 0.5 s. We cannot unambiguously experimentally determine whether these fluctuations are spatial or temporal. If they are interpreted as purely spatial structures, a typical 1-2 s spike would have a spatial extent perpendicular to the magnetic field along the plasma sheet normal of 4-40 km and the duration of the spike in the rest frame of plasma could be much longer than 1 s. Alternatively, the spikes could be a temporal structure lasting ~ 1 s in the rest frame of the plasma with a spatial scale perpendicular to the plasma sheet much larger than the 4-40 kms scales in the previous scenario. In fact, the perpendicular scales could range up to the large spatial scales (1500-7000 km) discussed in the previous paragraph.

Estimated characteristic scale sizes and frequencies of the plasma sheet derived from measured density, ion and electron temperature, and magnetic field strength are summarized for the May 9, 1997 event in Table 1. The values for the May 1 event are similar. For the measured 0.4 cm^{-3} density of electrons (Plate 1), the Debye length λ_{De} is about 40 m. The magnitude of the measured magnetic field of 400 nT and typical ion and electron energies in the keV range yield an ion gyroradius (ρ) of about 22 km and an electron gyroradius of 0.3 km. The ion acoustic gyroradius is given by $\rho_S = (kT_e/m_i)^{1/2}/\omega_{ci}$~ 15 km. The electron inertial length, c/ω_{Pe} is ~10 km. All electric field scale sizes discussed above are much larger than a Debye length and larger than the electron gyroradius. The largest spatial scales of 1500-7000 km are much larger than the local ion gyroradius, and the electron inertial length. However, if 1 s spikes are interpreted as spatial structures with scale sizes of 4-40 km, then their scale sizes are comparable to (or smaller than) the electron inertial length and the ion gyroradius. The general dispersion relation [*Lysak and Lotko*, 1996; *Stretslov and Lotko*, 1995; and references therein] including both finite gyroradii effects and electron inertial effects may be approximated by

Table 1. Plasma Parameters* PSBL (May 9, 1997)

Plasma Parameter	Experimental Value
Plasma density	0.3 cm^{-3}
Magnitude B	400 nT
f_{CH+}	6 Hz
f_{CO+}	0.4 Hz
Mean energy ions	4 keV
Mean energy electrons	2 keV
Debye length	25 m
c/ω_{PO+}	1720 km
c/ω_{PH+}	430 km
c/ω_{pe}	10 km
r_{Li} (H+)	22 km
r_{Le}	.3 km
Beta	0.001
Alfven velocity (100% H^+)	12,000 km/s
Ion acoustic speed (H^+)	450 km/s

*On plasma sheet side of crossing derived from Hydra and MFE key parameters.

$$\omega^2 = V_A^2 k_\parallel^2 (1 + k_\perp^2 \rho_s^2) /(1+ k_\perp^2 c^2/\omega_{pe}^2)$$

Thus small-scale structures with $k_\perp\rho_S$, $k_\perp c/\omega_{pe} \geq 1$ are governed by a dispersion relation depending on the perpendicular as well as the parallel wave number. Under these circumstances the group velocity and Poynting flux may have a significant component perpendicular to the magnetic field. These waves may carry electromagnetic energy to adjacent auroral flux tubes and broaden the layer of Poynting flux as it propagates to lower altitudes. This could provide a mechanism which broadens the latitudinal spatial extent of auroral acceleration. Small perpendicular scale waves also develop parallel components of the electric field which are parallel to the magnetic field which can accelerate electrons to form beams and also dissipate Alfven wave energy [*Hasegawa*, 1976; *Goertz*, 1984; *Lysak*, 1990; *Lysak and Lotko*, 1996]. Two parameters are important in understanding the propagation of the waves. The ratio of electron thermal energy density to magnetic field energy density β_e and the ratio of ion to electron thermal temperature control whether there is significant Landau damping of the waves. At the edge of the plasma sheet, β_e is ~.001 which is comparable to m_e/m_i the electron to ion mass ratio. The Hydra measurements also indicate the ratio of ion to electron temperature is Ti/Te~2. For these latter two conditions the analysis and simulations of *Lysak and Lotko* [1996], and references therein, indicate that that small scale Alfven structures may undergo Landau damping and thereby accelerate electrons through small parallel electric fields. For the plasma parameters discussed, the ratio of the damping frequency to the wave frequency is between .05 to 0.3.

8. Discussion and Conclusions

In this paper, measurements of electric and magnetic fields and particle fluxes by instruments on the Polar spacecraft at geocentric distances of 4-6 R_E above the auroral acceleration region were used to characterize the properties of very large-amplitude electric fields and the associated Poynting flux near the outer boundary of the plasma sheet.

Although large-amplitude spiky electric fields have previously been measured at the outer boundary of the plasma sheet at more distant positions in the geomagnetic tail by the electric field instrument on the ISEE-1 spacecraft [*Cattell et al.*, 1982; *Pedersen* et al., 1985], the two pair of electric probes on ISEE-1 were deployed in the equatorial plane and could not measure the component of the electric field normal to the plasma sheet. In the Polar data set this normal component is measured and (along with the associated magnetic field perturbations) often produces the dominant contributions to the Poynting flux.

Measurements of the Poynting flux toward the Earth from the geomagnetic tail have never been measured at altitudes above the auroral acceleration region. Consequently, there have never been comparisons of this Poynting flux to estimates of the energy necessary to power the auroral acceleration processes (particularly the energization of electron beams). The in situ measurements obtained from the Polar spacecraft along with its capability of providing ultraviolet images of the aurora allow us to assess for the first time the role of Poynting flux from the tail in powering auroral particle acceleration. Similarly, although one of the central features of substorm dynamics is the explosive release of magnetic field energy stored in the tail and its conversion to particle energy in the form of intense ion flows and particle heating in the plasma sheet, the role of Poynting flux as a major component of the energy released during this explosive process has never been experimentally assessed. The experimental data presented in this paper suggest that Poynting flux in the form of intense Alfven waves at the boundary of the plasma sheet can be an important way for energy to be transported away from the reconnection region.

The two electric field events presented herein were obtained from a data set of about 25 plasma sheet crossings containing the largest electric field structures seen in one year (1997) of Polar plasma sheet crossings (about 400 orbits). These two plasma sheet crossings have been chosen to be representative of these intense electric field events, but in fact, these plasma sheet crossings contain a rich diversity of plasma and field phenomenology and cannot be characterized entirely by any two events. We note, however, that most of the large electric field structures observed in the Polar data set are directly or indirectly related to auroral dynamics. For example, a statistical analysis using 24 months of Polar data shows that the spatial distribution of high-altitude, large-amplitude electric fields (>20 mV/m) delineates the average boundary of the auroral oval [*A. Keiling et al.*, manuscript in preparation, 2000] in a manner similar to the distribution of the "electrostatic shocks" observed by S3-3 at ~1 R_E altitude in the auroral acceleration region [*Bennett et al.*, 1983].

The electric fields for the two events presented herein are polarized predominantly perpendicular to the nominal plasma sheet boundary and reach amplitudes >100 mV/m. The associated magnetic field perturbations lie primarily in the plane of the plasma sheet and are orthogonal to the local magnetic field. Individual fluctuations have durations in the spacecraft frame between 1 s and 30 s (where the electric field data was averaged over 1/2 s). The Poynting flux associated with these fields ranges up to values exceeding several ergs cm^{-2} s^{-1} at altitudes of about 5 R_E and is usually directed earthward. When mapped to 100 kms altitude, assuming converging magnetic field lines, the mapped value of the Poynting flux (assuming dissipationless propagation) exceeds 100 ergs cm^{-2} s^{-1}. The strongest values of Poynting flux are generally confined to thin layers which the spacecraft encounters for periods of 1-3 min. These layers of strong electromagnetic energy flux coincide with locally observed signatures of lower-altitude particle acceleration which include intense flows of upgoing field-aligned ions and also electron beams flowing both parallel and antiparallel to the magnetic field. The observed layers of strong Poynting flux occur at times and places magnetically conjugate to the positions at 100 km altitude where the Ultraviolet Imager on Polar observes strong deposition of energy in the ionosphere due to accelerated auroral electron beams. Typical peak values of the energy flux associated with the electron beams as inferred from the UVI images range between 15-30 ergs cm^{-2} s^{-1}. This fact is strong evidence that the Poynting flux due to Alfven waves is responsible for the powering of auroral acceleration processes. In addition, in a separate unpublished study, we have found that in the absence of strong Poynting flux, the auroral emission (and the inferred energy deposition due to electron beams) as determined from UVI is weak. We have investigated the UV images for Polar plasma sheet crossings which have small electric fields (<5mV/m), small perturbations in the magnetic field, and low values of Poynting flux (< 0.05 ergs cm^{-2} s^{-1}). Under those circumstances we find that the energy flux associated with magnetically conjugate auroral electron beams as inferred by the UV images was < 1 erg/cm^2s. This is further evidence that Poynting flux incident is a necessary condition for powering the aurora. Examples of these passes will be presented in a forthcoming paper. Preliminary results from the analysis of the rest of the orbits in the data set of 25 plasma sheet crossings at about 5 R_E altitude obtained during 1997 associated with intense electric fields indicate that the peak value of the Poynting flux is earthward and exceeds 0.5 ergs cm^{-2} s^{-1} in about 70% of these crossings.

The ratio of the peak perturbation electric to magnetic fields from the May 1, 1997, and the May 9, 1997, crossings is consistent with wave phase velocities of 4000 to 10000 km/s. These velocities are in the range of the locally determined Alfven velocity. The ratio of electric to magnetic fields is 2 orders of magnitude larger than c/Σ_P which is the ratio associated with steady state electric fields and associated field-aligned current structures closing in the ionosphere in the absence of parallel potential drops. This indicates that the dominant contribution to the Poynting flux is due to large-amplitude Alfven waves. The magnitudes of the parallel Poynting flux incident on the Earth due to Alfven waves, as presented herein, exceed by 1-2 orders of magnitude typical values of the "steady state" Poynting flux derived from the convection electric fields and the large-scale field-aligned current system.

Although electric and magnetic field wave forms are quite similar (Plate 1), closer inspection (Figure 2a) shows that they are sometimes phase shifted relative to each other. This phase shift is evidence that the electric and magnetic field wave forms are a superposition of downward and upward Alfven waves. The fact that the Poynting flux is generally earthward indicates that the downward propagating waves are usually more intense that the upward propagating waves. However, there are sometimes instances when the upward waves dominate. For example, there is a brief time interval during the May 1, 1997, event in which the net Poynting flux is upward.

The geometry of these electric and magnetic field fluctuations is similar to the shear mode Alfven surface waves first proposed by *Hasegawa* [1976] as a mechanism for powering the aurora. For example, in the May 9, 1997, event the surface waves were immediately adjacent to the plasma sheet tail lobe density jump on the high-density plasma sheet side. In the May 1, 1997, plasma sheet crossing, there was no apparent density jump near the waves.

These observations presented herein are strong evidence that Poynting flux due to Alfven waves is an important if not dominate supplier of the power dissipated in the acceleration of auroral electron beams. The observations indicate that Alfven waves are a major mechanism at ~5 R_E altitude for transporting energy from the tail to the ionosphere. These observations further suggest that Poynting flux associated with large-amplitude Alfven waves may be a significant energy sink for energy release processes in the tail such as reconnection, since in our examples, the Poynting flux at Polar spacecraft altitudes was comparable or larger than the total energy flux due to electrons and ions. Thus in terms of understanding the energetics of the reconnection process itself, in addition to producing accelerated jets of ions, the reconnection region may radiate a large energy flux of Alfven waves which couples comparatively directly to auroral acceleration processes.

Acknowledgments. The authors would like to thank the two referees for a number of useful comments. Analysis of electric field data was supported by NASA International Solar Terrestrial Program (NASA contract NAG 5-3182). Work at the University of Washington was supported by NASA grant NAG 5-3170. Analysis of magnetometer data was supported by NASA ISTP grant 5-3217. Work at Lockheed-Martin Palo Alto Research Laboratory (W.K.P.) was supported by contract NAS5-30302. Work at the University of Iowa in analysis of Hydra data was performed under NASA grant NAG 5 2231 and DARA grant 50 OC 8911 0. The results of the Hydra investigation were made possible by the decade-long hardware efforts of groups led at NASA GSFC by K. Ogilvie, at UNH by R. Torbert, at MPAe by A. Korth, and UCSD by W. Fillius. We would also like to thank Reiner Friedel and coworkers for use of the PAPCO graphical display program.

Hiroshi Matsumoto thanks M.C. Kelley and another referee for their assistance in evaluating this paper.

References

Bennett, E.C., et al, Distribution of auroral electrostatic shocks below 8000-km altitude, *J. Geophys. Res.*, *88*, 7107, 1983.

Block, L.P., and C.-G. Falthammer, Role of magnetic-field-aligned electric fields in auroral acceleration, *J. Geophys. Res.*, *95*, 5877-5888, 1990.

Carlson, C. W., R. F. Pfaff, and J. G.Watzin, Fast Auroral Snapshot (FAST) mission, *Geophys. Res. Lett.*, *25*, 2013, 1998.

Cattell, C.A., Comparisons of Polar satellite observations of solitary wave velocities in the Plasma Sheet Boundary Layer and the high-altitude cup to the auroral zone, *Geophys. Res. Lett.*, *26*, 425, 1999.

Cattell, C. A., M. Kim, R. P. Lin, and F. Mozer, Observations of large electric fields at the Plasma Sheet Boundary Layer by ISEE-1, *Geophys. Res. Lett.*, *9*, 539, 1982.

Eastman, T.E., L. A. Frank, W.K. Peterson, and W. Lennartsson, Plasma Sheet Boundary Layer, *J. Geophys. Re.*, *89*, 1553, 1984.

Ergun, R. E., et al., Fast satellite observations of electric field structures in the auroral zone, *Geophys. Res. Lett.*, *25*, 2025, 1998.

Fairfield, D. H., Structure of the geomagnetic tail, in *Magnetotail Physics*, edited by A. T. Lui, p 23, Johns Hopkins Univ. Press, Baltimore, Md., 1987.

Germany, G. A., et al., Auroral observations from the Polar Ultraviolet Imager (UVI), in *Results from International Solar Terrestrial Physics Program, Geophysical Monogr. Ser.* vol. 104, pp. 108, AGU, Washington, D. C., 1998.

Ghielmetti, A. G., et al., Downward flowing ions and evidence for injection of ionospheric ions into the plasma sheet, *J. Geophys. Res.*, *84*, 156, 1979.

Goertz, C.K., Kinetic Alfven waves on auroral field lines, *Planet. Space Sci.*, *32*, 1387, 1984.

Harvey, P., et al., The Electric Field Instrument on the Polar satellite, in *The Global Geospace Mission*, p 583, edited by C.T. Russell, Kluwer Acad., Norwell, Mass., 1995.

Hasegawa, A., Particle acceleration by MHD surface wave and formation of the aurora, *J. Geophys. Res.*, *81*, 5083, 1976.

Kelley, M. C., J. A. Starr, and F.S. Mozer, Relationship between the magnetospheric electric field and the motion of auroral forms, *J. Geophys. Res.*, *76*, 5269, 1971.

Kelley, M.C., D. J. Knudsen, and J.F. Vickery, Poynting flux measurements on a satellite: A diagnostic tool for space research, *J. Geophys. Res.*, *96*, 201-207, 1991.

Kletzing, C., G. Berg, M. C. Kelley, F. Primdahl, and R. B. Torbert, Electrical and percipitation characteristics of morning sector Sun-aligned auroral arc, *J. Geophys. Res*, *101*, 17,175, 1996.

Louarn, E., et al, Observation of kinetic Alfven waves by the FREJA spacecraft, *Geophys. Res. Lett.*, *21*, 17, 1847, 1994.

Lyons, L.R., Discrete auroral and magnetotail processes in *Auroral Physics*, edited by C.-I. Meng, M.J. Rycroft, and L. A. Frank, pp. 195-205, Cambridge Univ. Press, New York, 1991.

Lysak, R.L., Electrodynamic coupling of the magnetosphere and ionosphere, *Space Sci. Rev.*, *52*, 33, 1990.

Lysak, R. L., and W. Lotko, On the dispersion relation for shear Alfven waves, *J. Geophys. Res.*, *101*, 5085, 1996.

Lysak, R.L., Relationship between electrostatic shocks and kinctic Alfven waves, *Geophys. Res. Lett.*, *25*, 2089, 1998

Maynard N.C., W. J. Burke, E.M. Basinska, G. M. Erickson, W. J.Hughes, H. J. Singer, A. J. Yahnin, D.A. Hardy, and F. S. Mozer, Dynamics of the inner magnetosphere near times of substorm onset. *J. Geophys. Res.*, *101*, 7705, 1996

McFadden, J.P., et. al., Spatial structure and gradients of ion beams observed by FAST, *Geophys. Res. Lett.*, *25*, 2021, 1998.

Mozer, F.S., et al, Observations of paired electrostatic shocks in the polar magnetosphere, *Phys. Rev. Lett.*, *38*, 292-295, 1977.

Mozer, F.S., et al, Satellite measurements and theories of low-altitude auroral particle acceleration, *Space Sci. Rev*, *27*, 155-213, 1980.

Mozer, F.S. et. al., New features of time domain electric field structures in the auroral acceleration region, *Phys Rev Lett.*, *79*, 1281, 1997.

Nagatsuma, T., et al., Field-aligned currents associated with Alfven waves in the poleward boundary region of the nightside auroral oval, *J. Geophys. Res.*, *101*, 21,715, 1996.

Pedersen, A., et al., Electric fields in the plasma sheet and plasma sheet boundary layer, *J. Geophys. Res, 90,* 1231, 1985.

Reiff, P.H., et al., On the high- and low-altitude limits of the auroral electric field region in *Auroral Plasma Dynamics, Geophys. Monogr. Ser.* Vol. *80*, edited by R.L. Lysak, p. 143, AGU Washington, D.C. 1993.

Russell, C.T., R.C. Snare, J.D. Means, D. Pierce, D. Dearborn, M. Larson, G. Barr, and G. LE, The GGS/Polar Magnetic Fields Investigation, in *The Global Geospace Mission*, p 563, edited by C. T. Russell, Kluwer Acad., Norwell, Mass., 1995.

Scudder, J., et al., A 3-dimensional electron and ion hot plasma instrument for the Polar spacecraft of the GGS mission, in *The Global Geospace Mission*, p 495, edited by C. T. Russell, Kluwer Acad., Norwell, Mass., 1995.

Stenbaek-Nielsen, H.C., et al., Aircraft observations conjugate to FAST: Auroral arc thickness, *Geophys. Res. Lett.*, **25**, 2073, 1998.

Streltsov A. V. and Lotko W., Dispersive Field Line Resonances on Auroral Field Lines, *J. Geophys. Res.., 100*, 19457, 1995.

Temerin, M. C., Cattell, R. Lysak, M. Hudson, R. B. Torbert, F. S. Mozer, R. D. Sharp, and P. M. Kintner, Small-scale structure of electrostatic shocks, *J. Geophys. Res.*, *86*, 11,278, 1981.

Torr, M.R., et al., A Far Ultraviolet Imager for the International Solar Terrestrial Physics Mission, in *The Global Geospace Mission*, edited p 329, by C.T. Russell, Kluwer Acad., Norwell., Mass., 1995.

Weimer, D.R., and D.A. Gurnett, Large-amplitude auroral electric fields measured with DE 1, *J. Geophys. Res., 98*, 13,557, 1993.

Williams, D. J., Energetic ion beams at the edge of the plasma sheet: ISEE observations plus a simple explanatory model, *J. Geophys. Res., 86*, 5507, 1981.

Zelenyi, L. M., R.A. Kovrazkhin, and J.M. Bosqued, Velocity dispersed ion beams in the night side auroral zone: AUREOL 3 observations, *J. Geophys. Res.*, *95,* 12,119, 1990.

M. Brittnacher and G. Parks, Geophysics Program, University of Washington, Seattle, WA 98195.

C. A. Cattell, M. Johnson, A. Keiling, R. L. Lysak, and J. R. Wygant, School of Physics and Astronomy, University of Minnesota, Minneapolis, MN 55455. (wygant@ham.space.umn.edu)

G. Germany and J. Spann, NASA Marshall Space Flight Center, Huntsville, AL 35812.

C. A. Kletzing and J. D. Scudder, Department of Physics and Astronomy, University of Iowa, Iowa City, IA 52242.

F. S. Mozer and M. Temerin, Space Sciences Laboratory, University of California, Berkeley, CA 94720.

W. Peterson, Lockheed-Martin Palo Alto Laboratories, Palo Alto, CA 94304.

C. T. Russell, Institute of Geophysics and Planetary Physics, University of California, Los Angeles, CA 90024.

(Received March 29, 1999; revised December 1, 1999;
accepted December 8, 1999.)